Frequency-domain Block Signal Detection with QRM-MLD for Frequency-domain Filtered Single-carrier Transmission

Tetsuya YAMAMOTO† Kazuki TAKEDA† and Fumiyuki ADACHI‡
Dept. of Electrical and Communication Engineering, Graduate School of Engineering, Tohoku University
6-6-05 Aza-Aoba, Aramaki, Aoba-ku, Sendai, 980-8579 Japan
†{yamamoto, kazuki}@mobile.ecei.tohoku.ac.jp, ‡adachi@ecei.tohoku.ac.jp

***Abstract*—The frequency-domain filtered single-carrier (SC) signal transmission can achieve improved bit error rate (BER) performance due to additional frequency diversity gain while keeping a lower peak-to-average power ratio (PAPR) property than orthogonal frequency division multiplexing (OFDM). In this paper, we extend our recently proposed frequency-domain block signal detection (FDBD) with MLD employing QR decomposition and M-algorithm (QRM-MLD) to the frequency-domain filtered SC block transmissions. QR decomposition is applied to a concatenation of the transmit filter, propagation channel, and discrete Fourier transform (DFT). We evaluate BER and throughput performances by computer simulation. From performance evaluation, we discuss how the filter roll-off factor affects the achievable BER and throughput performances and show that as the filter roll-off factor increases, the required number of surviving symbol-candidates in the M-algorithm can be reduced.**

Keywords-component; SC, frequency-domain filtering, QRM-MLD, frequency-domain signal detection

I. INTRODUCTION

In next generation mobile communication systems, broadband data services are demanded. Since the broadband channel is composed of many propagation paths with different time delays, the channel becomes severely frequency-selective [1]. The single-carrier (SC) transmission with frequency-domain equalization (FDE) has good bit error rate (BER) performance [2, 3] and low peak-to-average power ration (PAPR) property. Therefore, the SC with FDE is advantageous for the uplink applications [4].

In many practical wireless systems, transmit filtering is used to limit the signal bandwidth. When a square-root Nyquist filter is used, the roll-off factor α ($0 \le \alpha \le 1$) is the design parameter of the transmit filter [5]. When $\alpha=0$, the SC signals have smaller PAPR than orthogonal frequency division multiplexing (OFDM) signals [6] while keeping the same signal bandwidth [7, 8]. As α increases, the PAPR further decreases at the cost of increased bandwidth [9]. FDE based on the minimum mean square error criterion (MMSE-FDE) can make use of this increased bandwidth to obtain larger frequency diversity gain and improve the BER performance [10]. However, the performance improvement is limited due to the presence of residual inter-symbol interference (ISI) after MMSE-FDE. There is still a big performance gap from the theoretical lower bound (the matched filter (MF) bound).

The maximum likelihood detection (MLD) is an optimal detection, but it requires a prohibitively large computational complexity. MLD employing QR decomposition and M-algorithm (called QRM-MLD) is known as a complexity efficient MLD [11]. Recently, we proposed a frequency-domain block signal detection (FDBD) with QRM-MLD for the reception of SC signals transmitted over a frequency-selective channel [12]. QR decomposition (QRD) is applied to a concatenation of the propagation channel and discrete Fourier transform (DFT). We showed [12] that the FDBD with QRM-MLD can achieve the BER performance close to the MF bound while considerably reducing the computational complexity compared to the MLD.

By viewing a concatenation of the transmit filter, propagation channel, and DFT as an equivalent channel, FDBD with QRM-MLD can be extended to the frequency-domain filtered SC signal transmission. Larger frequency diversity gain is achieved by exploiting the excess bandwidth introduced by the transmit filter. In this paper, we develop QRM-MLD for the reception of the filtered SC signals and investigate the BER and throughput performances by computer simulation. We discuss how the filter roll-off factor affects the achievable BER and throughput performances and the required number of surviving symbol-candidates in the M-algorithm. 1

II. FDBD WITH QRM-MLD FOR FREQUENCY-DOMAIN FILTEREED SC TRANSMISSION

A. Transmission System

The system model of the frequency-domain filtered SC signal transmission using FDBD with QRM-MLD is illustrated in Fig. 1. At the transmitter, a binary information sequence is data-modulated and then, the data-modulated symbol sequence is divided into a sequence of signal blocks $\{d(n); n=0\sim N_m-1\}$ of N_m symbols each, where N_m is the number of symbol per block. The data symbol block is transformed by N_m-point DFT into the frequency-domain signal $\{D(k); k=-N_m/2\sim N_m/2-1\}$, which is then, expanded to the frequency-domain signal $\{S(k); k=-(1+\alpha)N_m/2\sim(1+\alpha)N_m/2-1\}$ by applying the frequency-domain transmit filter with the roll-off factor α. Finally, N_c-point inverse DFT (IDFT) is applied to obtain the filtered time-domain transmit block $\{s(t); t=0\sim N_c-1\}$. The last N_g samples of transmit block are copied as a cyclic prefix (CP) and inserted into the guard interval (GI) placed at

978-1-4244-3574-6/10/$25.00 ©2010 IEEE

the beginning of each transmit block and a CP-inserted filtered signal block of N_c+N_g samples is transmitted.

The filtered SC signal block is transmitted over a frequency-selective fading channel. The received signal block after GI removal is transformed by N_c-point DFT into the frequency-domain signal $\{Y(k);\ k=-N_c/2\sim N_c/2-1\}$. Then, FDBD with QRM-MLD is carried out to obtain the decision variable block. In this paper, a representation using discrete time normalized by the DFT (also IDFT) sampling period T_c is used.

B. Transmit Signal Representation

The data symbol block of N_m symbols is expressed using the vector form as $\mathbf{d}=[d(0),\ldots,d(n),\ldots,d(N_m-1)]^T$. $\mathbf{d}$ is transformed by N_m-point DFT into the frequency-domain signal $\mathbf{D}=[D(-N_m/2),\ldots,D(k),\ldots,D(N_m/2-1)]^T$ as

$$\mathbf{D}=\mathbf{F}^{(N_m)}\mathbf{d}, \tag{1}$$

where $\mathbf{F}^{(J)}$ is the DFT matrix of size $J\times J$ given by

$$\mathbf{F}^{(J)}=\frac{1}{\sqrt{J}}\begin{bmatrix} 1 & e^{\left(-j2\pi\frac{-J/2\times 1}{J}\right)} & \cdots & e^{\left(-j2\pi\frac{-J/2\times(J-1)}{J}\right)} \\ 1 & e^{\left(-j2\pi\frac{(-J/2+1)\times 1}{J}\right)} & \cdots & e^{\left(-j2\pi\frac{(-J/2+1)\times(J-1)}{J}\right)} \\ \vdots & \vdots & \ddots & \vdots \\ 1 & e^{\left(-j2\pi\frac{(J/2-1)\times 1}{J}\right)} & \cdots & e^{\left(-j2\pi\frac{(J/2-1)\times(J-1)}{J}\right)} \end{bmatrix}. \tag{2}$$

$\mathbf{D}$ is transformed the frequency-domain filtered signal $\mathbf{S}=[S(-(1+\alpha)N_m/2),\ldots,S(k),\ldots,S((1+\alpha)N_m/2-1)]^T$ as

$$\mathbf{S}=\mathbf{H}_T\mathbf{D}, \tag{3}$$

where $\mathbf{H}_T$ is $(1+\alpha)N_m\times N_m$ transmit filter matrix given by

$$\mathbf{H}_T=\begin{bmatrix} & & & & & & H_T\left(-\frac{(1+\alpha)N_m}{2}\right) & & \mathbf{0} \\ & & & & & & & \ddots & \\ & & & & & & & & H_T\left(-\frac{N_m}{2}-1\right) \\ H_T\left(-\frac{N_m}{2}\right) & & & & & & & & \\ & \ddots & & & & \mathbf{0} & & & \\ & & \ddots & & & & & & \\ & & & & H_T(0) & & & & \\ & & & & & \ddots & & & \\ & & & & & & \ddots & & \\ & & & & \mathbf{0} & & & & H_T\left(\frac{N_m}{2}-1\right) \\ H_T\left(\frac{N_m}{2}\right) & & & & & & & & \\ & \ddots & & & & & & & \\ \mathbf{0} & & H_T\left(\frac{(1+\alpha)N_m}{2}-1\right) & & & & & & \end{bmatrix}. \tag{4}$$

where $H_T(k)$, $k=-(1+\alpha)N_m/2\sim(1+\alpha)N_m/2-1$, represents the transmit filter transfer function. $S(k)$ is given as

$$S(k)=\begin{cases} H_T(k)D(k+N_m) & -\frac{(1+\alpha)N_m}{2}\le k\le -\frac{N_m}{2}-1 \\ H_T(k)D(k) & -\frac{N_m}{2}\le k\le \frac{N_m}{2}-1 \\ H_T(k)D(k-N_m) & \frac{N_m}{2}\le k\le \frac{(1+\alpha)N_m}{2}-1 \end{cases}. \tag{5}$$

Finally, N_c-point IDFT is applied to obtain the time-domain signal block $\mathbf{s}=[s(0),\ldots,s(t),\ldots,s(N_c-1)]^T$ as

$$\mathbf{s}=\sqrt{2E_s/T_s}\,\mathbf{F}^{(N_c)H}\widetilde{\mathbf{S}}, \tag{6}$$

where E_s and T_s are respectively the transmit symbol energy and duration, $(.)^H$ is the Hermitian transpose operation, and $\widetilde{\mathbf{S}}=[\widetilde{S}(-N_c/2),\ldots,\widetilde{S}(k),\ldots,\widetilde{S}(N_c/2+1)]^T$ given by

$$\widetilde{\mathbf{S}}=[0,\ldots,0,S\left(-\frac{(1+\alpha)N_m}{2}\right),\ldots,S(k),\ldots,S\left(\frac{(1+\alpha)N_m}{2}-1\right),0,\ldots,0]^T. \tag{7}$$

The IFDT block size N_c at the transmitter can be $N_c\ge(1+\alpha)N_m$. In this paper, we use the N_c-point IDFT irrespective of the value of α.

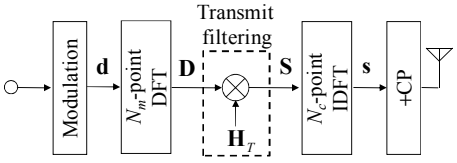

(a) Transmitter

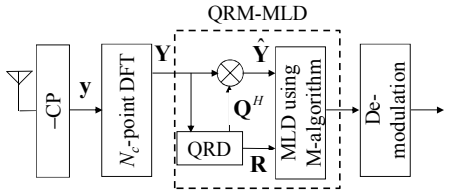

(b) Receiver

Figure 1. System model of the SC transmission using frequency-domain filtering and FDBD with QRM-MLD.

C. Received Signal Representation

We assume an L-path block fading channel. The channel impulse response $h(\tau)$ can be represented as

$$h(\tau)=\sum_{l=0}^{L-1}h_l\delta(\tau-\tau_l), \tag{8}$$

where h_l and τ_l are respectively the complex-valued path gain with $E[\sum_{l=0}^{L-1}|h_l|^2]=1$ and the time delay of the lth path. We assume that the normalized time delay of the lth path is l, i.e. $\tau_l=l$. The GI-removed received signal block $\mathbf{y}=[y(0),\ldots,y(t),\ldots,y(N_c-1)]^T$ can be expressed using the vector form as

$$\mathbf{y}=\sqrt{2E_s/T_s}\,\mathbf{h}\mathbf{s}+\mathbf{n}, \tag{9}$$

where $\mathbf{h}$ is the $N_c\times N_c$ channel impulse response matrix given as

$$\mathbf{h}=\begin{bmatrix} h_0 & & & & & h_{L-1} & & h_1 \\ h_1 & h_0 & & & & & \ddots & \vdots \\ \vdots & h_1 & h_0 & \mathbf{0} & & & & h_{L-1} \\ h_{L-1} & \vdots & h_1 & \ddots & & & & \\ & h_{L-1} & \vdots & & h_0 & & & \\ & & h_{L-1} & & h_1 & \ddots & & \\ \mathbf{0} & & & \ddots & \vdots & & & h_0 \end{bmatrix}, \tag{10}$$

and $\mathbf{n}=[n(0),...,n(t),...,n(N_c-1)]^T$ is the noise vector. The tth element, $n(t)$, of $\mathbf{n}$ is the zero-mean complex Gaussian variable having the variance $2N_0/T_c$ with N_0 being the one-sided power spectrum density of the additive white Gaussian noise (AWGN).

D. FDBD with QRM-MLD

The received signal block $\mathbf{y}$ is transformed by N_c-point DFT into the frequency-domain signal $\mathbf{Y}=[Y(-N_c/2),\ldots,Y(k),...,Y(N_c/2-1)]^T$. $\mathbf{Y}$ is expressed as

$$\mathbf{Y} = \mathbf{F}^{(N_c)}\mathbf{y} = \sqrt{2E_s/T_s}\mathbf{F}^{(N_c)}\mathbf{h}\mathbf{s} + \mathbf{F}^{(N_c)}\mathbf{n}. \quad (11)$$

Due to the circulant property of $\mathbf{h}$ [13], we have

$$\mathbf{F}^{(N_c)}\mathbf{h}\mathbf{F}^{(N_c)H} = diag[H(-N_c/2),\ldots,H(k),...,H(N_c/2-1)] \equiv \mathbf{H}_c, \quad (12)$$

where $H(k)=\sum_{l=0}^{L-1}h_l\exp(-j2\pi k\tau_l/N_c)$, k=$-N_c/2$~$N_c/2-1$. Using Eqs. (1), (3), (6), (7), and (12), the frequency-domain received signal $\tilde{\mathbf{Y}}=[Y(-(1+\alpha)N_m/2),...,Y(k),...,Y((1+\alpha)N_m/2)]^T$ to be used in FDBD with QRM-MLD can be expressed as

$$\tilde{\mathbf{Y}} = \sqrt{\frac{2E_s}{T_s}}\tilde{\mathbf{H}}_c\mathbf{H}_T\mathbf{F}^{(N_m)}\mathbf{d} + \tilde{\mathbf{N}} = \sqrt{\frac{2E_s}{T_s}}\overline{\mathbf{H}}\mathbf{d} + \tilde{\mathbf{N}}, \quad (13)$$

where $\tilde{\mathbf{H}}_c = diag[H(-(1+\alpha)N_m/2),\ldots,H(k),...,H((1+\alpha)N_m/2-1)]$ and $\tilde{\mathbf{N}}=[N(-(1+\alpha)N_m/2),...,N(k),...,N((1+\alpha)N_m/2)]^T$ is the frequency-domain noise vector. $\overline{\mathbf{H}}=\tilde{\mathbf{H}}_c\mathbf{H}_T\mathbf{F}^{(N_m)}$ is an equivalent channel matrix of size $(1+\alpha)N_m\times N_m$. From Eq. (13), FDBD with QRM-MLD can also be applied to the frequency-domain filtered SC transmission by treating a concatenation of transmit filter, frequency-domain propagation channel, and DFT as an equivalent channel.

QRM-MLD is composed of three steps. Firstly, we apply the QRD to $\overline{\mathbf{H}}$ to obtain $\overline{\mathbf{H}}=\mathbf{Q}\mathbf{R}$, where $\mathbf{Q}$ is a $(1+\alpha)N_m\times N_m$ matrix satisfying $\mathbf{Q}^H\mathbf{Q}=\mathbf{I}$ ($\mathbf{I}$ is the identity matrix) and $\mathbf{R}$ is an $N_m\times N_m$ upper triangular matrix. In the case of SC transmission, all symbols have the same signal-to-interference plus noise power ratio (SINR) and hence, no ordering is necessary.

Secondly, by multiplying $\mathbf{Q}^H$ to frequency-domain received signal $\tilde{\mathbf{Y}}$, we have the transformed vector

$$\hat{\mathbf{Y}} = \mathbf{Q}^H\tilde{\mathbf{Y}} = \sqrt{2E_s/T_s}\mathbf{R}\mathbf{d} + \mathbf{Q}^H\tilde{\mathbf{N}}. \quad (14)$$

Thirdly, MLD using the M-algorithm [11] is carried out. Thanks to the upper triangular structure of $\mathbf{R}$, MLD has a tree structure of N_m stages and therefore, the M-algorithm can be applied to reduce the computational complexity. In the nth stage, the path metric is computed using the squared Euclidean distance for a candidate sequence of $d(N_m-1-n)$~$d(N_m-1)$ as

$$e_n = \left|\hat{Y}(N_m-1-n) - \sqrt{\frac{2E_s}{T_s}}\sum_{i=0}^{n}R_{N_m-1-n,N_m-1-i}\bar{d}(N_m-1-i)\right|^2, \quad (15)$$

where $R_{k,i}$ is the (k, i) the element of matrix $\mathbf{R}$ and $\bar{d}(n)$ is the candidate symbol for $d(n)$. Then, the sum of path metrics until the nth stage is computed as $E_n=\sum_{n'=0}^{n}e_{n'}$. The best M candidate sequences are selected as surviving symbol-candidates by comparing the sum metrics for all candidates and are passed to the next stage. The sum metrics computation and selection of M best symbol-candidates are repeated until the last stage. At the last stage, the data demodulation is carried out by tracing back the path arriving at the symbol-candidate having the smallest sum metric.

III. Computer Simulation

The simulation condition is shown in Table 1. We consider 16QAM data modulation, N_m=64, and N_c=128. The square-root raised cosine Nyquist filter with roll-off factor α is used. The channel is assumed to be a frequency-selective block Rayleigh fading channel having L=16-path uniform power delay profile and the normalized time delay $\tau_l=l$. Ideal channel estimation is assumed.

TABLE I. Computer Simulation Condition

Transmitter	Modulation	16QAM
	Number of symbols per block	N_m=64 symbols
	DFT/IDFT size	N_c=128 samples
	CP length	N_g=16 samples
Transmit filter	Transfer function	Square-root raised cosine
Channel	Fading type	Frequency-selective block Rayleigh
	Power delay profile	L=16-path uniform power delay profile
	Time delay	$\tau_l=l$ (l=0~L–1)
Receiver	Signal detection	FDBD with QRM-MLD, MMSE-FDE
	Channel estimation	Ideal

A. BER Performance

The average BER performance of the frequency-domain filtered SC transmission using FDBD with QRM-MLD is plotted for various values of M in Fig. 2 as a function of average received bit energy-to-noise power spectrum density ratio E_b/N_0(=$(E_s/N_0)(1+N_g/N_c)/4$). For comparison, the BER performance using MMSE-FDE [10] and the MF bound [14] are also plotted. It is seen from Fig. 2 that FDBD with QRM-MLD provides significantly improved BER performance compared to the MMSE-FDE. By increasing the value of M, BER performance close to the MF bound is obtained. Furthermore, as α increases, better BER performance can be achieved even if small M is used. This is because by using excess bandwidth, larger frequency diversity gain can be obtained and accordingly, the probability of removing the correct symbol-candidates at the early stages can be reduced similar to the antenna diversity case [12].

How increasing α reduces the probability of removing the correct symbol-candidates at the earlier stages is discussed. Fig. 3 plots the sum of the probability of removing correct symbol-candidates at the 0th, 1st, 2nd, and 3rd stages when E_b/N_0=12dB. As α increases, the probability of removing the correct symbol-candidates at the early stages can be reduced.

Figure 4 plots the required M so that the E_b/N_0 gap from the MLD for achieving BER=10^{-3} become 1.8 dB. When α=0, M=256 is required. However, when α=0.5 and 1.0, much smaller M (i.e., M=32 and M=4) is required. As a result, by increasing α, the computational complexity of FDBD with QRM-MLD can be reduced at the cost of increased bandwidth.

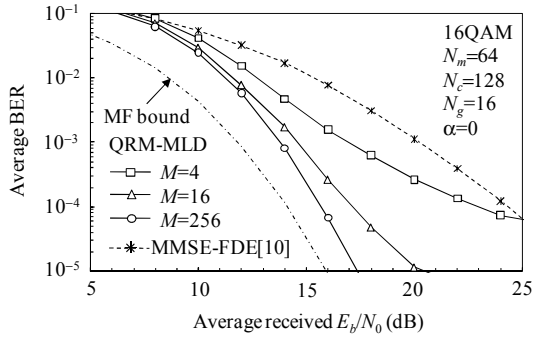

(a) α=0

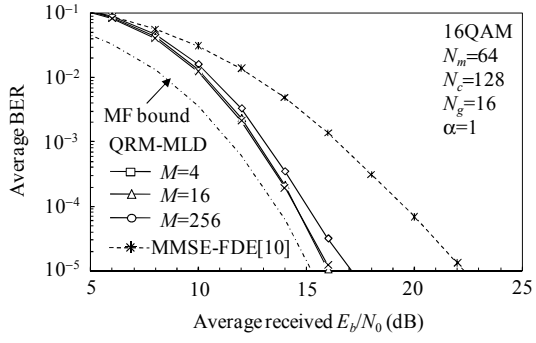

(b) α=1.0

Figure 2. BER performance.

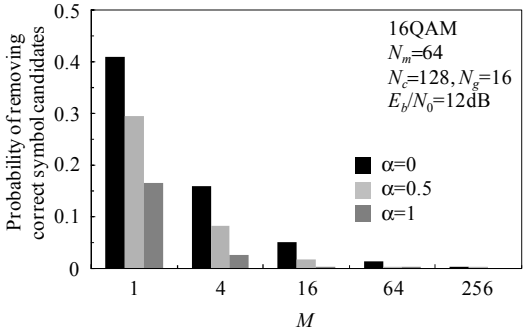

Figure 3. Probability of removing correct symbol-candidates at earlier stages.

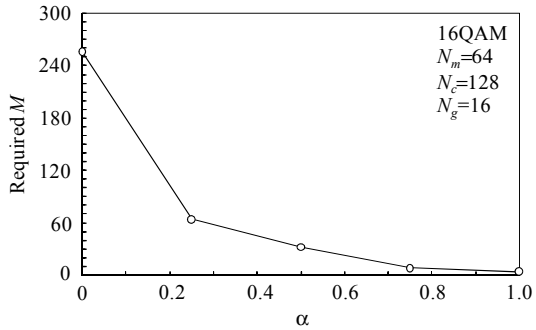

Figure 4. Required E_b/N_0 as a function of α

We discuss the overall computational complexity, which is the sum of the complex multiply operations required for DFT, QRD, multiplication of $\mathbf{Q}^H$, and the squared Euclidean distance calculation. When the DFT size at a receiver is J, the number of complex multiplications is J^2 for DFT (if J is power of 2, $J\log_2 J$ for FFT). The number of complex multiplications is $(1+\alpha)N_m^3$ for QRD, $(1+\alpha)N_m^2$ for the multiplication of $\mathbf{Q}^H$, and $2X + XM\sum_{n=1}^{N_m-1}(n+2)$ for the squared Euclidean distance calculations. As the filter roll off factor α increases, higher complexity is required for QRD and multiplication of $\mathbf{Q}^H$ (this is because the size of equivalent channel matrix $\overline{\mathbf{H}}$ becomes large). However, as α increases, the complexity required for the squared Euclidean distance calculations is significantly reduced because the required M can be reduced as mentioned above. As a result, the overall complexity reduces. When 16QAM is used, filtered SC transmission with α=0.5(1.0) reduces the computational complexity to about 22(25) % of the case α=0.

B. Throughput Performance

The throughput performance is plotted for various values of M in Fig. 5 as a function of average received E_s/N_0. The throughput η(bps/Hz) is defined as

$$\eta = \log_2 X \times (1-\mathrm{PER}) \times \frac{1}{1+\alpha} \times \frac{1}{1+N_g/N_c}, \qquad (16)$$

where PER is the packet error rate. In this paper, packet transmission of size 1024 bits is assumed. For comparison, the throughput performance using MMSE-FDE [10] is also plotted in Fig. 5. FDBD with QRM-MLD can significantly improve the throughput performance compared to the MMSE-FDE. Furthermore, by increasing the value of M, sufficiently improved throughput performance is achieved. Furthermore, as α increases, sufficiently improved throughput performance can be achieved even if small M is used.

Figure 6 plots the throughput as a function of M when the peak E_s/N_0=25dB. Peak E_s/N_0 is defined as the average received E_s/N_0 plus $\mathrm{PAPR}_{0.1\%}$ value (the measured PAPR distribution is shown in Appendix). As α increases, smaller M is required to achieve sufficiently improved throughput. It can also be seen from Fig. 6 that in low peak E_s/N_0 region (peak E_s/N_0=25dB), when M is smaller than 4, the throughput increases as α increases and the maximum throughput is obtained when α=1. This is because by increasing α, larger frequency diversity gain can be obtained. On the other hand, when M is large enough (e.g., $M\geq$16), the throughput is maximized when α=0.5. This is because when M is large enough, sufficiently improved throughput can be achieved even when α is small, however, the PAPR level becomes almost the same beyond α=0.5.

IV. CONCLUSION

In this paper, we developed a computational efficient FDBD with QRM-MLD for filtered SC signal reception. QRD is applied to a concatenation of transmit filter, propagation channel, and DFT. We showed that FDBD with QRM-MLD can significantly improve the BER and throughput performances compared to the MMSE-FDE. Furthermore, we showed that as α increases, better BER performance can be achieved even if small M is used. As a result, by increasing α, the computational complexity of FDBD with QRM-MLD can be reduced at the cost of increased bandwidth. We also showed that in the low peak E_s/N_0 region, when M is small, the throughput increases as α increases and the maximum throughput is obtained when α=1. On the other hand, when M is large enough, the throughput is maximized when α=0.5.

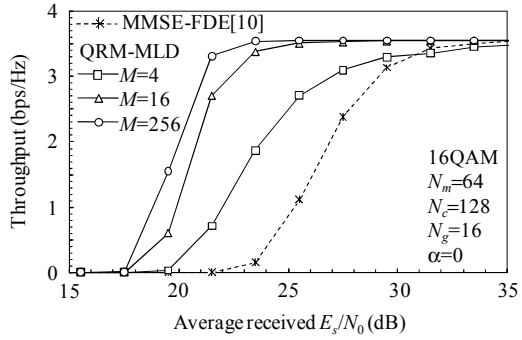

(a) α=0

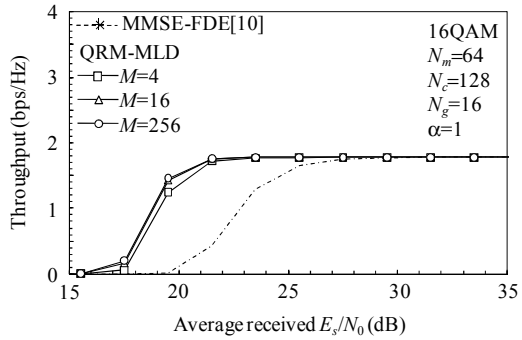

(b) α=1.0

Figure 5. Throughput performance.

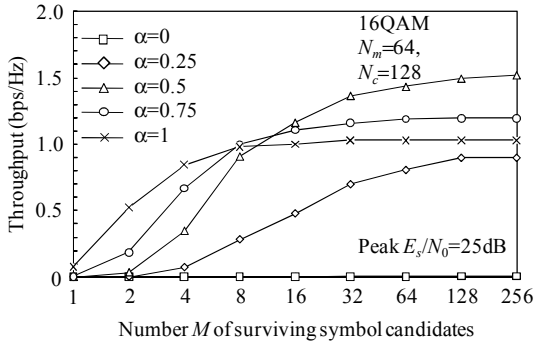

Figure 6. Throughput versus M.

REFERENCES

[1] J. G. Proakis and M. Salehi, *Digital communications*, 5th ed., McGraw-Hill, 2008.

[2] D. Falconer, S. L. Ariyavisitakul, A. Benyamin- Seeyar B. Edison, "Frequency domain equalization for single-carrier broadband wireless systems," IEEE Commun. Mag., Vol. 40, No. 4, pp. 58-66. Apr. 2002.

[3] K. Takeda, T. Itagaki, and F. Adachi, "Joint use of frequency-domain equalization and transmit/receive antenna diversity for single-carrier transmissions," IEICE Trans. Commun., vol. E87-B, No. 7, pp.1946-1953, Jul. 2004.

[4] H. Ekstrom, A. Furuskar, J. Karlsson, M. Meyer, S. Parkvall, J. Torsner, and M. Wahlqvist, "Technical solutions for the 3G long-term evolustion," IEEE Commun. Mag., Vol. 44, No. 3, pp. 38-45, Mar. 2006.

[5] Y. Akaiwa, Introduction to digital mobile communication, Wiley, Newyork, 1997.

[6] R. Van Nee, and R. Prasad, *OFDM for Wireless Multimedia Communications*, Artech House, 2000.

[7] H. G. Myung and D. J. Goodman, *Introduction to single carrier FDMA: A new air interface for long term evolution*, John Wiley & Sons Inc, 2008.

[8] V. Tarokh and H. Jafarkhani, "On the computation and reduction of the pear-to-average power ratio in multicarrier communications," IEEE Trans. Commun., Vol. 48, No. 1, pp. 37-44, Jan. 2000.

[9] S. Daumont, B. Rihawi, and Y. Lout, "Root-raised cosine filter influences on PAPR distribution of single carrier signals," The 2nd International Symposium on Communications, Control and Signal Processing (ISCCSP 2008), pp. 841-845, Malta, Mar. 2008.

[10] S. Okuyama, K. Takeda, and F. Adachi, "MMSE frequency-domain equalization using spectrum combining for Nyquist filtered broadband single-carrier transmission," to be presented at The 71st Vehicular Technology Conference (VTC2010-Spring), Taiwan, May 2010.

[11] L. J. Kim and J. Yue, "Joint channel estimation and data detection algorithms for MIMO-OFDM systems," in Proc. Thirty-Sixth Asilomar Conference on Signals, System and Computers, pp. 1857-1861, Nov. 2002.

[12] T. Yamamoto, K. Takeda, and F. Adachi, "Single-carrier transmission using QRM-MLD with antenna diversity," The 12th International Symposium on Wireless Personal Multimedia Communications (WPMC 2009), Japan, Sept. 2009.

[13] G. H. Golub and C. F. van Loan, *Matrix Computations*, 3rd ed. Baltimore, MD, Johns Hopkins Univ. Press, 1996.

[14] F. Adachi and K. Takeda, "Bit error rate analysis of DS-CDMA with joint frequency-domain equalization and antenna diversity combining," IEICE Trans. Commun., Vol. E87-B, No. 10, pp.2991-3002, Oct. 2004.

APPENDIX

The complementary cumulative distribution function (CCDF) of the PAPR is plotted in Fig. 7 for both the frequency-domain filtered SC and OFDM. 16QAM is used. It is seen from Fig. 7 that as α increases, the PAPR level of filtered SC signals decreases, but it is kept almost the same beyond α=0.5.

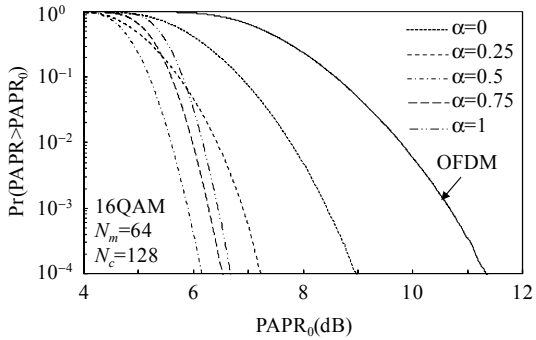

Figure 7. PAPR distribution.